A TOROIDAL MAGNET OPTION

J.P. Cussonneau, H. Gutbrod, P. Lautridou, L. Luquin, V. Métivier, V. Ramillien

Laboratoire SUBATECH, UMR Université, Ecoles des Mines, IN2P3/CNRS, F-44070 Nantes Cedex 03, France

Abstract

The possibility of using, for the ALICE forward muon spectrometer, a superconducting toroidal magnet has been considered in place of the SC dipole. The study has been restricted to the acceptance calculations and to the tracking simulations of the toroidal magnet but without technical investigations. The estimated performances are found maladjusted to the physics requirements of the heavy ion runs.

1 introduction

The design of the ALICE forward spectrometer has to be optimized in order to measure the complete spectrum of the heavy quark resonances J/ψ, ψ', Υ, Υ' and Υ'', via their muonic decay in pp, Ca-Ca and Pb-Pb collisions. The magnetic analyser is one of the most important part of the detector since, in a first look, the physic acceptance and the momentum resolution are linked to the magnet opening and the field integral. Two constraints have to be kept in mind to adjust the magnet parameters:

- Due to the limited production rate of the Υ' and the Υ'' in the Pb-Pb runs, the acceptance should be in the range of 5 % to 10 % which transforms into an aperture of 10° to 18°.

- For a clear separation between the Υ' and the Υ'' signal, the mass resolution in the Υ region needs to stay in all accessible kinematical regions below 100 MeV.

A toroidal magnet option which could satisfy these requests is presented below.

2 Lay-out of the Toroidal Spectrometer

The general lay-out of the toroidal setup and its integration with the central detector is shown on figure 1. This lay-out is based on a modified version of the dipole setup given in the ALICE TP [1].

All material compositions (absorber, beam shielding, tracking chambers, etc..) are kept identical to the LOI [2], except the addition of the entrance and the exit windows needed for a SC toroidal magnet. The magnet geometry is based on that of the ATLAS End Cap Toroid [3] with an appropriate down-scaling in order to fit with the opening of the hole of the L3 iron yoke. The front of the magnet is set at 8 m from the vertex. For the GEANT simulations, it consists of a vacuum cylinder of 4 m length, 4 m outer radius and 0.3 m inner radius, which leads to an angular acceptance of $2^o < \theta < 18^o$. Below 2°, an iron cylinder inside the toroid surrounds the beam pipe down to 0.07 m radius. The SC magnet windows, which demarcate at each side the vacuum region inside the SC toroid, are materialized as aluminum skins of 4 % of radiation length each.

- Both sectant and octant shaped coils have been considered with aluminum coils of 0.25 m thickness. Cross-sections of the two internal toroidal geometries are sketched in figure 2.

In addition, two magnetic field topologies have been simulated.

- A first field option has been investigated, in the spirit of the NA10 set-up [4], with a 1/r radius dependence which expresses in (r,ϕ) polar coordinates as $\mathbf{B} = B_0 \, / \, r$ $\mathbf{e}_\phi$ with $B_0 = 0.6$ T. The deviation angle α writes: $\alpha_{dev} = B_0 \times ln(\frac{Z_{out}}{Z_{in}}) \times \frac{1}{P_T}$ with Z_{in} and Z_{out} the entrance and exit coordinates of the toroid.

- The second derivative only differs from the first one by the use of a constant field quite analogous to the ATLAS ECT. In this case, the used field has been defined as: $\mathbf{B} = B_0 \, \mathbf{e}_\phi$ with $B_0 = 0.6$ T ,which leads to a deviation angle in the form of: $\alpha_{dev} = B_0 \times (Z_{out} - Z_{in}) \times \frac{1}{P}$.

For the given value of B_0, the 1/r field will give, in principle, a better mass resolution above the rapidity y = 3 while the constant toroidal field will lead to a better magnetic integral for $\theta > 5.7^o$.

To take care of the magnet geometry, the chamber locations are moved at 5.25 m and 7.75 m for the two downstream stations, at 12.25 m and 15.75 m for the two upstream stations. The two tracking planes, used for the sagitta measurements inside the LOI dipole, are removed.

To take avantage of the toroid acceptance, the opening angle of the absorber is extended to 18°. Jointly, a slightly modified shape of absorber has been used in the angular region $10^o < \theta < 18^o$ (see figure 1). This modification was made necessary in order to avoid the increase of coulomb scattering due to an excess of absorber material at large angle. In the $2^o < \theta < 10^o$ region, the absorber stays identical to those of the LOI with 9 λ_I of

interaction length and 63 X_0 of radiation length. Above 10°, the absorber geometry is based on a troncate cone shape made of carbon which allows to reduce the interaction length and the radiation length to 5 λ_I and 10 X_0 respectively at 18°.

3   Tracking Performances

3.1   Simulation Overview

To estimate the tracking performances of the toroid setup, a chain of simulation and reconstruction programs has been developped using the modified dipole tracking codes. Calculations are based on GEANT for the set-up description and FORTRAN codes for the event generators and reconstruction procedures. All relevant physics processes are included in the simulation (e.g. multiple scattering, energy loss, bremsstrahlung, etc.). The following parameters are kept fixed for all tracking simulations:

- The diamond point is fixed at (0,0,0) for the particle emissions.

- The magnetic field is centered in the middle of the dimuon magnet and extends over the 4 m length of the toroid, leading to an integral field of 2.4 Tm at 1 m radius. Effect of the stray field has been calculated for the system L3+NA10 toroid. A negligible field perturbation was found [5]. This result was expected to be conservative in the case of our new foreseen toroids. Consequently, no stray field has been included and inside the L3 volume a pure solenoidal field is set to 0.2 T.

- The spatial measurement errors are introduced as gaussian smearing of the recorded hit positions from GEANT. In polar coordinates, the spatial resolution is set in the radial direction to $\sigma_r = 100$ μm and in the perpendicular direction to $\sigma_{r.\phi} = 1.4$ mm . The efficiency of the position detection has been fixed at 95 % per plane. Double hit effects were neglected.

- The muon stations are represented as aluminum sheets with a thickness of 2 % of radiation length per plane. Each tracking station is made of two (r,$r.\phi$) planes distant of 6 cm.

- For the resonance productions, the same physics event generators described in Ref. [6] have been used.

3.2   Mass Resolution

The tracking performances for the two toroidal fields have been estimated in the following way: tracks are analysed if the number of associated hits detected in the layers satisfies the minimum global majority of 3/4 for the upstream planes with 3/4 for the downstream planes. In a first step, a derivation of the muon momentum is searched not taking into account the absorber effects and the vertex location. The track fit is obtained by a chisquare minimization using the MINUIT package with five parameters : the transverse particle

3

momentum p_T, the two angles θ and ϕ which define the particle direction, and the two vertex coordinates x_V, y_V at $z_V = 0$. At the second step, the optimisation of the emission angle of the particles at the vertex is searched using a Branson correction [7]. A mean energy loss correction is applied to take care of the absorber material. At the end of this procedure, the final parameters of the particle at the emission vertex are derived. Due to the asymmetric nature of Landau fluctuations in energy loss, the reconstructed mass distribution of the resonnance exhibits a tail towards the low masses. Extraction of the resolution parameters is achieved using a Gaussian fit in the limits (-1.5 σ, +2.5 σ) around the maximum of the mass distribution. In this case, no more than 10 % of the resonance events populates the low mass tail below the 1.5 σ limit.

Rapidity and transverse momentum dependences of the mass resolution for the two field topologies are given in the figures 3 and 4 for both the $J/\psi's$ and the $\Upsilon's$.

Concerning the 1/r field, the mass resolutions have been calculated both for the for new absorber shape (troncated cone) and for a pur conical 18° absorber (in the way of the LOI) with a constant interaction length of 9 λ_I at all rapidities. In this last case,(start points in the Fig. 3), the Υ mass resolution can exceed 150 Mev due the large scattering in the rapidity region 1.8<Y<2.2 . The troncated absorber allows better resolutions versus the rapidity. But, due to the low field integral of the 1/r toroidal field at large angles, the resolution still reach 140 MeV at y=1.8 . As expected, both absorbers lead to the same mass resolution of 80 MeV at large rapidities. In the p_T plane, the Υ mean mass resolution is found around 110 MeV for the two absorbers with a slightly better dependance for the troncated absorber.

As stated previously, the motivation for the use of a constant toroidal field leads in the gain of resolution at large angle. However, to stay below the requested mass resolution of 100 MeV at high rapidity, the integral of the constant toroidal field has to be of the same order than the dipole one presented in the LOI. Figure 4 shows the rapidity and tranverse momentum dependences for the 0.6 T toroidal field using the troncated absorber shape. Dependence in rapidity of the mass resolution shows a clear improvement toward the low rapidities for which a mass resolution of 80 MeV is reached. As expected for the constant field, the mass resolution lowers to 100 MeV for Y > 3. When integrated over rapidities, the p_T dependence is slightly better of 10 MeV than the one observed for the 1/r field. Satisfactory performances are obtained in all domains of p_T and Y.

3.3 Acceptance

In order to estimate the integrated spectrometer acceptance, whole mind has been given to the magnet geometry for which both sectant and octant shaped coils have been considered. For the GEANT simulations, J/ψ's and Υ's are emitted in the apparatus. The correleted unlike sign muons are assumed to be detected only when they cross all the tracking stations. No attempt is done to impose futher impacts in the trigger layers and the muon energy threshold due to the trigger iron wall is not taken into account in the

acceptance calculations. In the same way, the effects of the p_T cuts at the trigger level have not been studied.

The figure 5 shows , for the sextant shape and the 0.6 T field, the obtained acceptance patterns in rapidity using the physical distributions of Ref. [6].

Due to the decrease of the available opening of the sextant shape at small angle, the acceptance of the J/ψ and the Υ strongly reduced at high rapidity. The maximum of acceptance is reached at rapidity y=2.6 with 35 % and 50 % of relative acceptance for the $J/\psi's$ and $\Upsilon's$ respectively. The total relative acceptances of the resonances, integrated over the total rapidity and transverse momentum distributions are summarised in table 3.3. The absolute acceptances of these onia are also given as indications.

	J/ψ	Υ
Relative Acceptance (%)	25.36	28.13
Absolute Acceptance (%)	3.42	3.81

Table 1: Relative and Absolute acceptance for J/ψ and Υ for the sextant shaped toroid with a constant field. The octant shape introduces another decrease of 0.3% in absolute acceptance. Equivalent results are obtained with the 1/r toroidal field.

3.4   Conclusion

All in all, compared to the constant toroidal field, the 1/r toroidal field seems less adapted in order to reach the requested mass resolution. Tracking performances obtained for the constant toroidal field seem equivalent to those of the dipole field [2]. However, from a trigger point of view, due to the field symmetry, a somewhat better trigger capabilities should advantage the toroids for which, experimentaly, a very easy p_T estimation of muons can be derived.

In spite of the large opening angle, the toroid acceptance is nearly two times smaller than the one of the 10° dipole (Ref. [2],Tab 1). This result is mainly due to the dead zones of the radial windings and it is estimated unsatisfactory in order to fullfil the physics goals.

Taking into account the financial cost of both the toroidal magnet and the large chambers needed to cover the opening angle, a dipole magnet could stand as a suitable option for the forward muon spectrometer.

References

[1] ALICE Technical Proposal, CERN/LHCC/95-71.

[2] ALICE Collaboration, Debye Screening in Heavy-Ion Collisions with the ALICE Detector, CERN/LHCC/95-24.

[3] ATLAS Technical Proposal, CERN/LHCC/94-43.

[4] L. Anderson et al. Nucl. Instr. Meth. 223 (1984) 26.

[5] D. Jouan and A. Lafoux, Private communication (1995).

[6] K. Eggert and A. Morsch, AT Group Report 95-01(DI) and ALICE Internal Note ALICE 95-05.
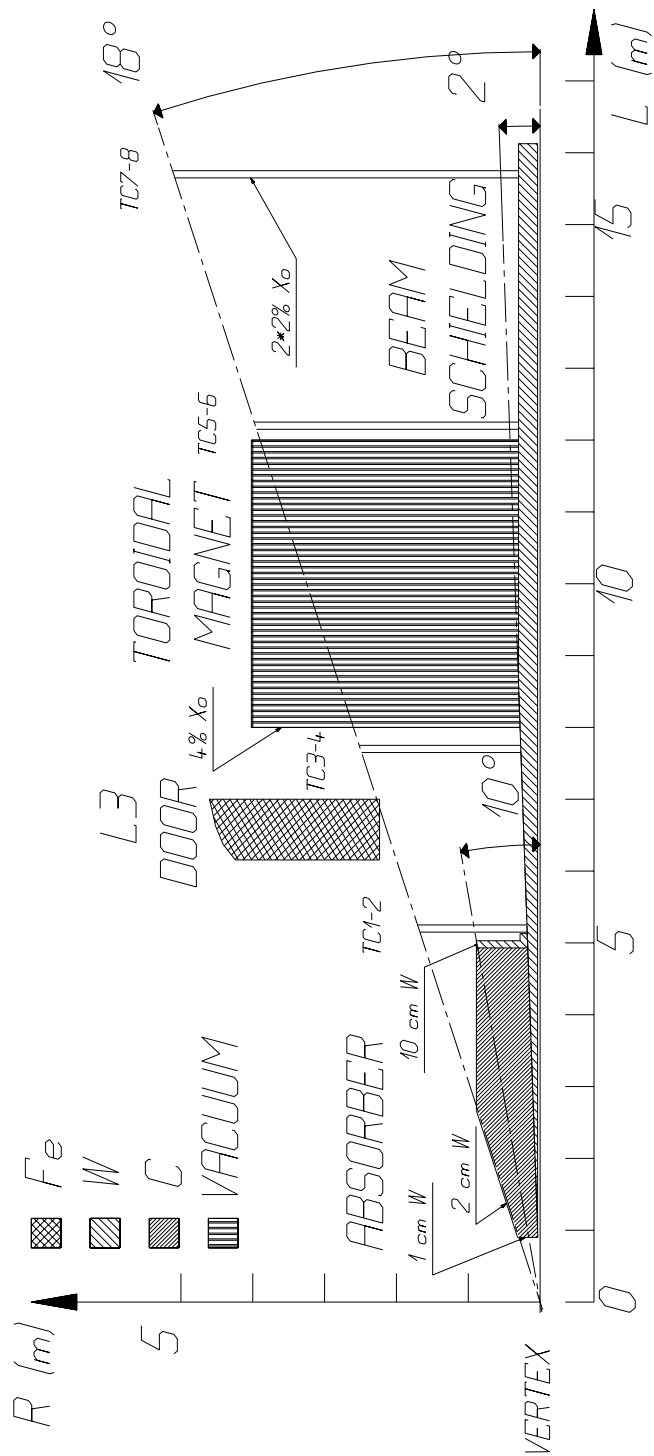
[7] J. G. Branson et al., Phys. Rev. Lett. 38 (1977) 1331.

Figure 1: Principal lay-out of the toroidal spectrometer and its integration in ALICE as used for the GEANT simulations with the modification of the absorber geometry for the low rapidity region.
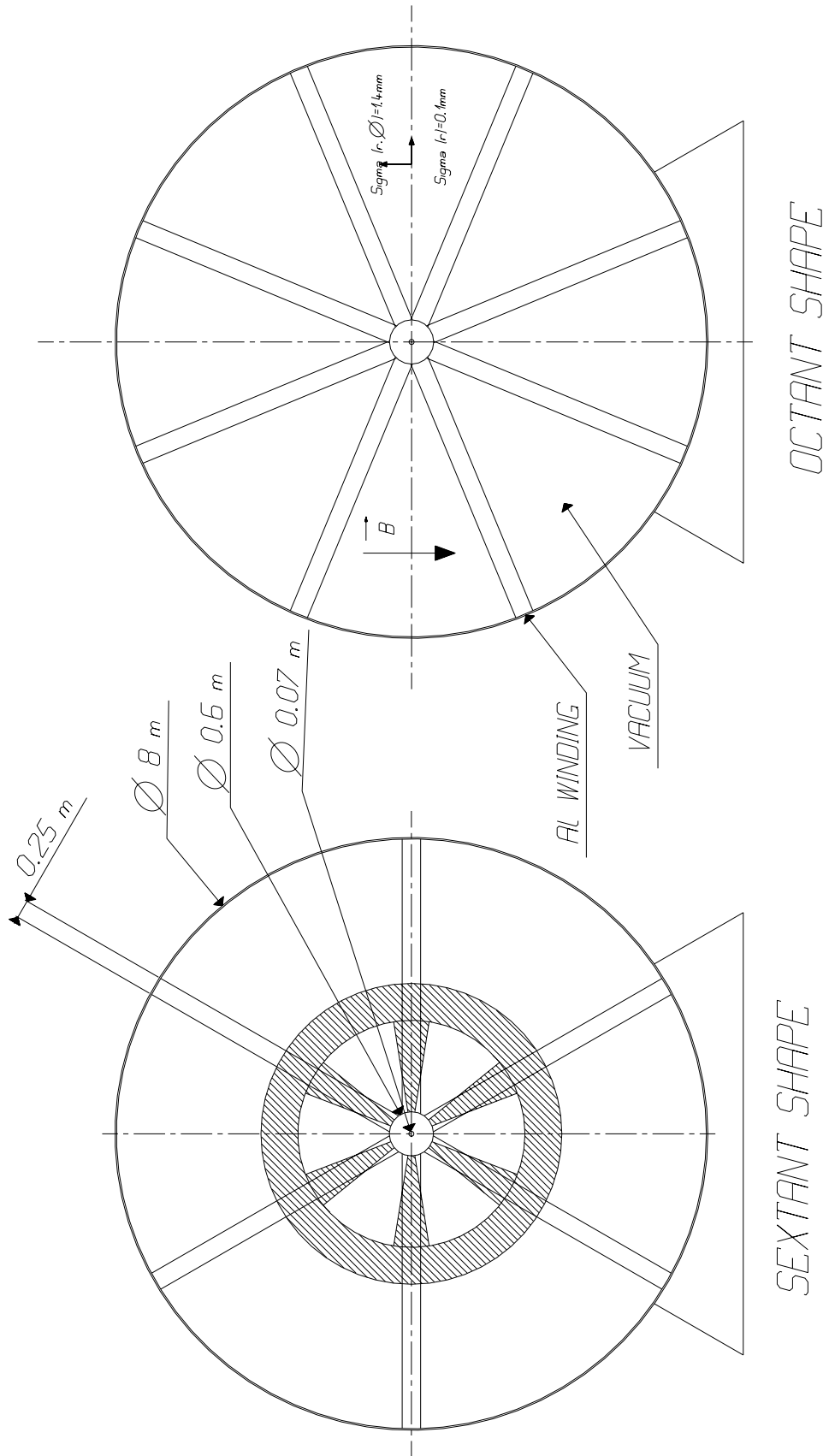
Figure 2: Principal lay-out of the toroid cross section for the sextant and octant shapes. Side view of the NA10 sextan toroid is drawn in hatched style for comparison.
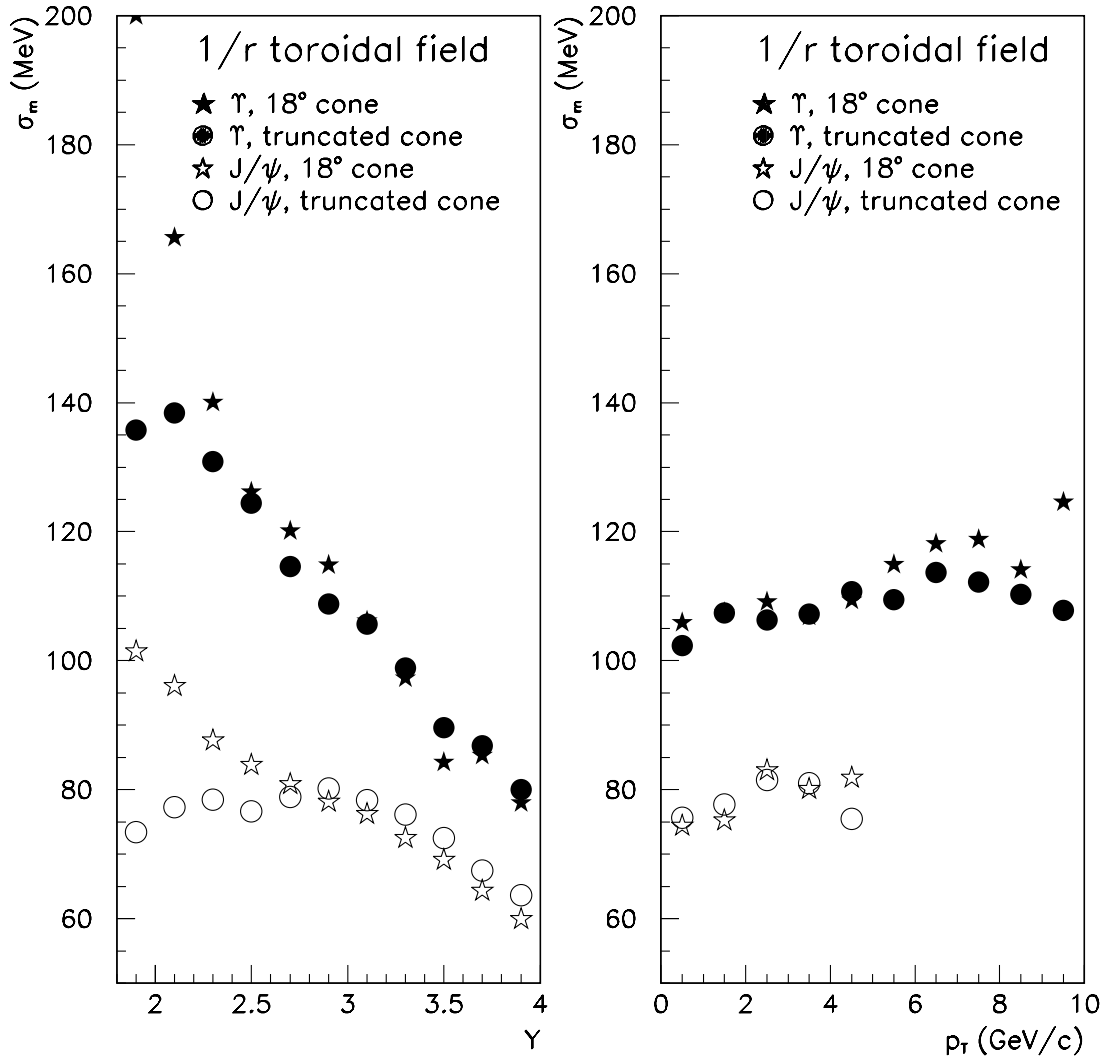
Figure 3: Mass resolution performance of the $J/\psi's$ and $\Upsilon's$ versus rapidity and transverse momentum for the 1/r toroidal field.
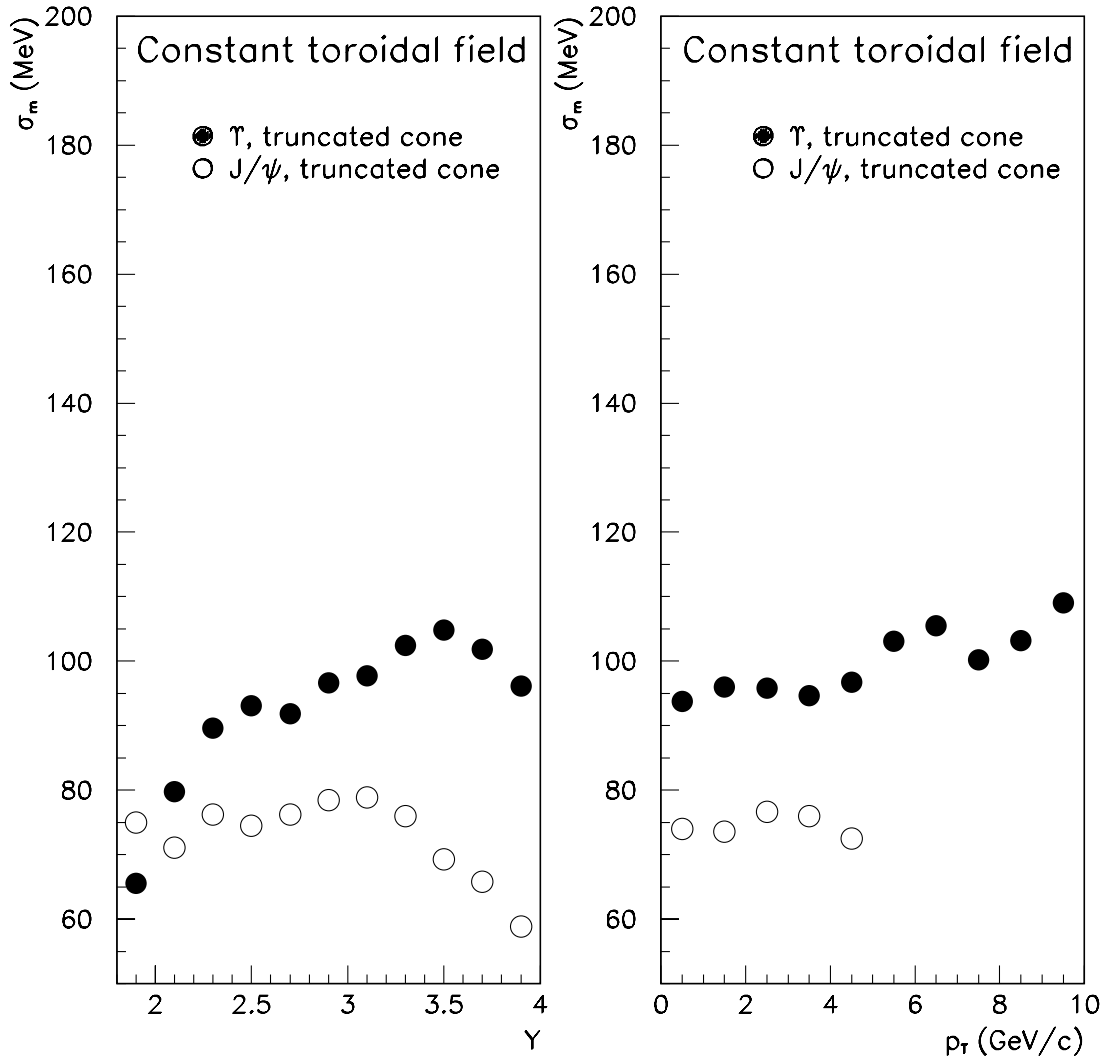
Figure 4: Mass resolution performance of the $J/\psi's$ and $\Upsilon's$ versus rapidity and transverse momentum for the constant toroidal field.
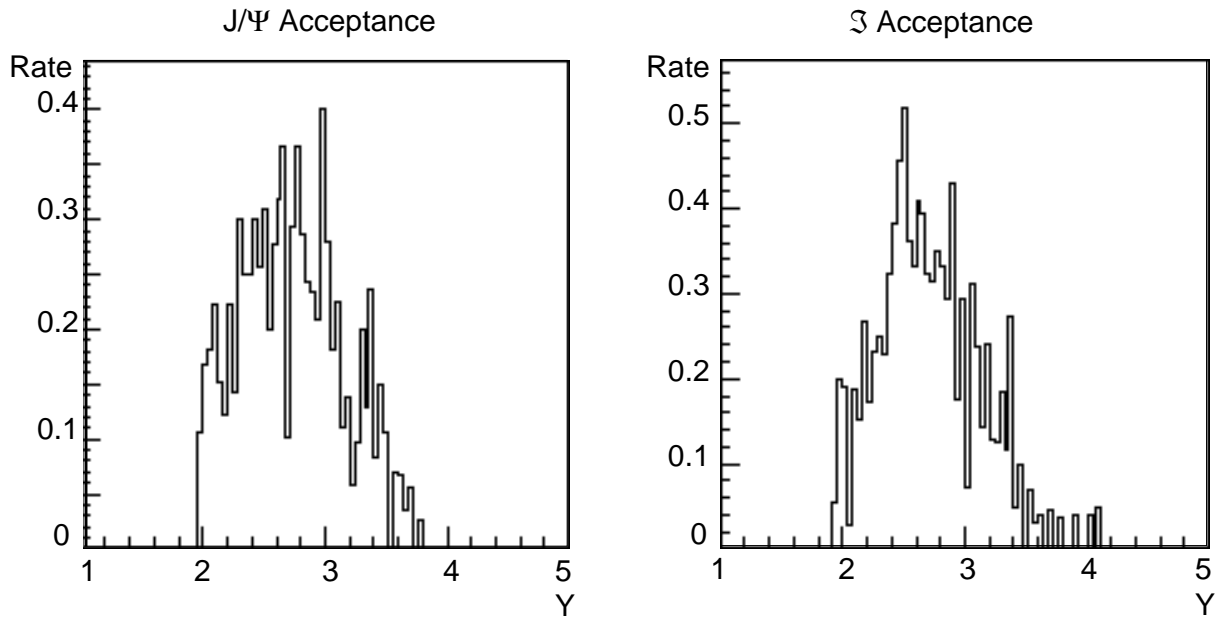
Figure 5: Pattern of the relative acceptances of the $J/\psi's$ and $\Upsilon's$ versus rapidity for the sextant toroid of constant field.